ELSEVIER

Journal of Volcanology and Geothermal Research 75 (1997) 337–358

Journal of volcanology and geothermal research

Spatial and temporal variations of volcanic earthquakes at Sakurajima Volcano, Japan

Kayoko Tsuruga [a,*], Kiyoshi Yomogida [a], Satoru Honda [a], Hisao Ito [b], Takao Ohminato [b], Hitoshi Kawakatsu [c]

[a] *Department of Earth and Planetary Systems Science, Faculty of Science, Hiroshima University, Higashi-Hiroshima 739, Japan*
[b] *Geological Survey of Japan, Tsukuba 305, Japan*
[c] *Earthquake Research Institute, University of Tokyo, Bunkyo-ku, Tokyo 113, Japan*

Received 24 October 1994; accepted 14 May 1996

Abstract

We conducted broadband seismic observations at three sites of the Sakurajima Volcano, Japan, from December 1992 to March 1993 in order to clarify the spatial and temporal variations of spectral properties of volcanic earthquakes: B-type earthquakes and volcanic tremor episodes. We used three STS-2 seismometers recording in the frequency range from 0.03 to 6 Hz. Major spectral peaks of both B-type earthquakes and volcanic tremor episodes are located in the frequency range of 1.1–1.3, 2.3–2.5 and 3.4–3.6 Hz. From the similarities of temporal variations in spectra among all the stations and of body-wave propagation in an early part of seismograms, spectral peaks of B-type earthquakes and volcanic tremor episodes mainly reflect source characteristics rather than site and path effects. Temporal variations of the dominant peaks are classified into three types for B-type earthquakes and into four types for volcanic tremor episodes. Two types of B-type earthquakes are similar to two of volcanic tremor episodes in terms of temporal variations of spectral peaks and of polarization characteristics with the only difference in amounts of energy. The similarities in the temporal variation of spectral properties indicate that B-type earthquakes and volcanic tremor episodes share common source mechanisms with different energy magnitudes. Since volcanic tremor episodes tend to take place prior to the swarms of B-type earthquakes and explosion earthquakes associated with any summit eruptions, we conclude that volcanic tremor episodes occur at the early stage of low-energy radiation, followed by B-type earthquakes as higher energy is radiated.

Keywords: Sakurajima Volcano; seismicity; volcanic earthquakes; temporal variations

1. Introduction

The Sakurajima Volcano, located in the southwest of Kyushu, Japan, is one of the most active volcanoes in the world. Volcanic and seismic phenomena at the Sakurajima Volcano have been observed and studied since 1910. The main subjects of seismic studies have been the relationship between volcanic earthquakes and volcanic activities (Kamo, 1978; Ishihara and Iguchi, 1989), temporal variations of spectral properties, polarizations of seismic waves, and phase velocities for either volcanic tremor episodes (e.g., Kakuta and Idegami, 1970; Kamo et al., 1977) or microearthquakes (e.g., Nishi, 1966;

* Corresponding author.

PII S0377-0273(96)00041-8

Kakuta and Nonaka, 1979; Iguchi, 1985). In those studies, analog recordings by classical seismometers with a natural period of about 1 s (e.g., Kakuta and Yoshiyama, 1977; Kamo et al., 1977; Nishi, 1978; Iguchi, 1985, 1994; Ishihara and Iguchi, 1989) were mainly analyzed so that seismic phenomena have been limited in a relatively high-frequency range (> 1–2 Hz).

Recently, STS-2 broadband seismometers are widely employed to monitor various kinds of seismic activities in global as well as regional problems. This seismometer has a flat and stable velocity response in the broad range of frequency, 1/120 to 50 Hz (e.g., Tsuruga et al., 1994). It is designed for portable installation with compact space, very useful for temporary observations. The use of broadband seismometers for earthquakes in volcanic areas has just started (Kawakatsu et al., 1992), showing it very effective for the monitoring of volcanic earthquakes because there are various kinds of events whose dominant frequency peaks are temporally variable over a wide range from 0.5 to more than 10 Hz.

In this paper, we analyze records of various earthquakes at the Sakurajima Volcano in a frequency range from 0.1 to 6 Hz at three stations. We study temporal and spatial variations of spectral properties to consider their possible causes, eventually to find out the relationship between volcanic earthquakes and volcanic tremor episodes.

2. Data

We conducted broadband seismic observations of volcanic earthquakes at the Sakurajima volcano from December, 1992 through March, 1993, under the initiative of the Geological Survey of Japan (Ohminato et al., 1993). We used Streckeisen STS-2 seismometers and Colombia DTC-8000 recorders with storage media of about 300 MB simultaneously at three sites: Arimura (ARM), Yunohira (YNH) and Koumen (KMN) as shown in Fig. 1. Our semi-continuous recording conditions were sampling rates of 50 Hz, pre-amp gain of 1 to 10, and anti-alias Bessel filters with a low-pass corner of 5–6 Hz. All the data were digitized by a 16-bit A/D converter and stored in magneto-optical disks in the field. After January 25, 1993, one more site, Kurokami (KKM), supplemented our observation sites by using an STS-2 seismometer and a Teledyne Geotech PDAS-100 recorder. Unlike other stations, event-trigger method was adopted with the sampling rate of 20 Hz and pre-amp gain of 10 to 100.

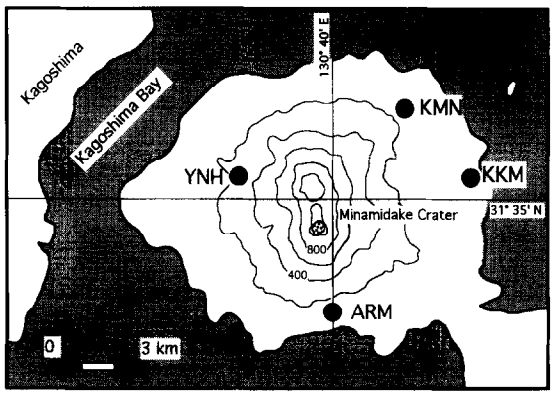

Fig. 1. Map of the Sakurajima Volcano and four observation sites: Arimura (ARM), Yunohira (YNH), Koumen (KMN) and Kurokami (KKM).

The recording sites, ARM, YNH, KMN and KKM, are located at horizontal distances of about 2.7, 2.9, 4.3 and 4.8 km from the recently active Minamidake crater, and at elevations of about 90, 370, 120 and 40 m above sea level, respectively. The geology of each site is variable: ARM located on the An-ei lava, YNH on the An-ei lava and the Yunohira pumice cone, KMN on the Minamidake lava and pyroclastics, and KKM on the Bunmei lava-II (Fukuyama and Ono, 1981; Aramaki and Kobayashi, 1986).

Volcanic earthquakes are classified into the following types: explosion, A-type, B-type earthquakes and volcanic tremor episode (e.g., Minakami, 1960) as shown in Fig. 2. In this paper, we define each earthquake type as follows: P and S waves can be clearly identified for *A-type earthquakes*, similar to tectonic earthquakes. *Volcanic tremor episodes* are continuous or intermittent vibrations for 10 s to several minutes with some characteristic spectral peaks and less distinct waveforms because of smaller amplitude than any other volcanic earthquakes (e.g., about $< 3 \times 10^{-5}$ m/s in the vertical component). One kind of microearthquakes generally occurs prior to *explosion earthquakes* that are associated with explosive summit eruptions. They consist of swarms with larger amplitude and more isolated waveforms

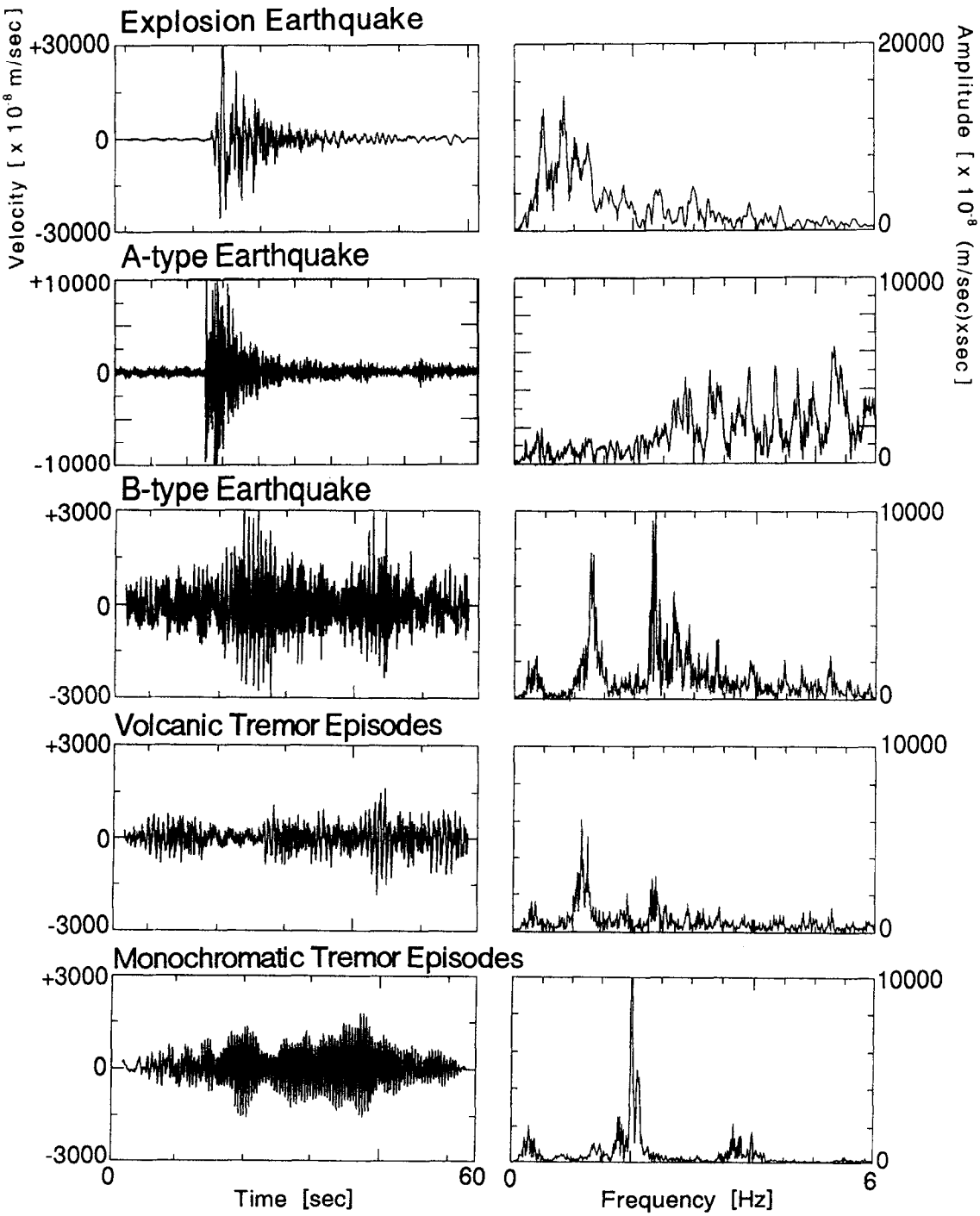

Fig. 2. Classifications of volcanic earthquakes. Typical velocity seismograms of explosion, A-type, B-type earthquakes and volcanic tremor episode recorded at ARM, and monochromatic tremor episode recorded at KMN.

than volcanic tremor episodes, which we call *B-type earthquakes*. They occasionally last for about 10–20 s. *Monochromatic tremor episode* with a spindle-shaped waveform has monochromatic spectral peaks, whose higher peak frequencies are integer multiples of the fundamental mode. Similar spectral characteristics are also recorded at other active volcanoes such as Langila Volcano, Papua New Guinea (Mori et al., 1989). In our analyzed data-set, amplitude of B-type earthquakes is about two to five times of that of volcanic tremor episodes in most cases. However, in some B-type earthquakes with small amplitude it is not easy to distinguish them from large volcanic tremor episodes only by the amplitude informations. In such a case, we refer other records of volcanic activities observed by the Japan Meteorological Agency at Kagoshima for checking our classifications.

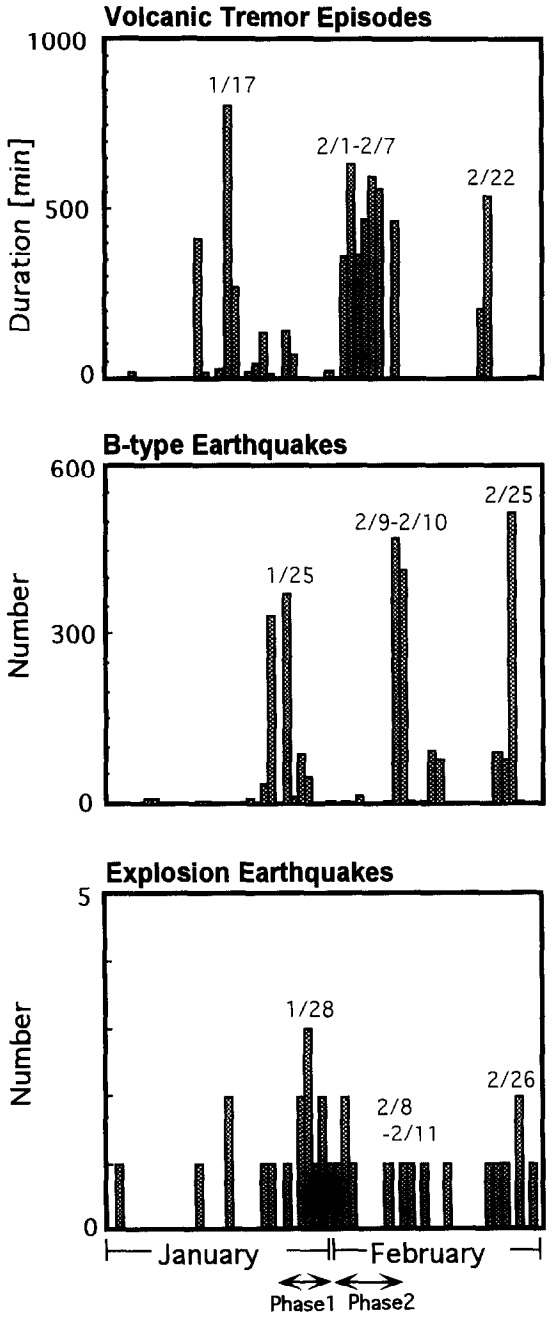

Fig. 3. Daily volcanic activities from January, 1 to February, 28, 1993. (a) Total durations time of volcanic tremor episodes, (b) the number of B-type earthquakes, and (c) the number of explosion earthquakes.

Table 1
Summary of observation (1)

Observation period	December, 1992–March, 1993 January, 1993–March, 1993 [a]
Observation site (distance from Minamidake Crater)	Arimura (ARM) (2.7 km) Yunohira (YNH) (2.9 km) Koumen (KMN) (4.3 km) Kurokami (KKM) (4.8 km) [a]
Recording system	STS-2 seismometer with DTC-8000 STS-2 seismometer with PDAS-100 [a]

[a] Event-trigger method detection

Kamo (1978) and Ishihara and Iguchi (1989) reported that some explosion earthquakes occur posterior to volcanic tremor episodes and B-type earthquakes. Fig. 3 shows the daily frequency (i.e., total duration-time) of volcanic tremor episodes, the total number of B-type earthquakes and that of explosion earthquakes from January 1 to February 28, 1993. Volcanic tremor episodes and swarms of B-type earthquakes occurred mainly in the following three periods: from January 12 to 25, from February 1 to 7 and from February 22 to 25. On the other hand, some explosion earthquakes occurred from January 27 to 31, February 9 to 11 and on February 26. In this study, we mainly used the data sets in two periods: from January 24 to 31, 1993 (phase-1) and February 1 to 10, 1993 (phase-2), as given in Tables 1 and 2 and shown in Fig. 3. These periods correspond to two active sequences in which volcanic tremor episodes and B-type earthquakes clearly occurred prior to explosion earthquakes. From the char-

Table 2
Summary of observation (2)

Analyzed phase	Phase 1 (93.1.24–93.2.6)	Phase 2 (93.2.6–93.2.10)
Sampling rate, pre-amp. gain	50 Hz, 1 ([a] 20 Hz, 10)	50 Hz, 10
Reliable frequency range	< 5–6 Hz ([a] < 7–8 Hz)	< 5–6 Hz

[*] Event-trigger method observation

acteristics of instruments and site conditions (e.g., Tsuruga et al., 1994; Tsuruga et al., 1995), the frequency ranges in which we can obtain high signal-to-noise ratio is from 0.1 to 6 Hz.

3. Source effects of volcanic earthquakes

It is well known that volcanic earthquakes have some unique spectral characteristics. For example, volcanic tremor episode has several dominant spectral peaks. In some cases, spectral peaks are located at a fundamental peak frequency and their higher-order frequencies (e.g., Kamo et al., 1977; Mori et al., 1989). The fundamental peak frequency of typical tremor episodes at Sakurajima Volcano, which varies with different time of volcanic activity, gradually increase from 0.5 to 1.3 Hz within a short time period (e.g., about 15 min), starting with shallow earthquakes and finishing with summit eruptions (Kamo et al., 1977). In contrast, B-type earthquakes have several spectral peaks in the frequency range from 1 to 5 Hz (i.e., BL-type earthquake) or from 5 to 8 Hz (i.e., BH-type earthquake) (Iguchi, 1989, 1994; Ishihara and Iguchi, 1989). The dominant frequency range varies temporally (Kakuta and Nonaka, 1979) and the spectrum tends to become monochromatic just before eruptions (Eto, 1988).

The origin of the above temporal variation of spectral peaks is still controversial: some researchers attribute it to the change of source spectra or source effect (e.g., Kamo et al., 1977; Schick et al., 1982; Iguchi, 1994), and others to the change of source locations or path effect (e.g., Minakami et al., 1957; Kakuta and Nonaka, 1979; Goldstein and Chouet, 1994). This problem is not easy because sub-surface structure in volcanic areas is highly complex and source mechanism of volcanic earthquakes may not be as simple as tectonic earthquakes that can be described well by a simple double-couple force. In this section, we shall clarify a most probable factor for the temporal variations of spectrals in our observation at Sakurajima Volcano.

Observed seismograms can be considered as an output of a series of linear filters, each of which corresponds to source, path or site factor. The effect of each factor can be eliminated by taking the spectral ratio between a particular pair of seismograms. For example, source factor can be isolated by taking the spectral ratio between seismograms recorded at a same station for two earthquakes with a common hypocenter and a similar some mechanism but different magnitudes (e.g., Berckhemer, 1962). At Sakurajima Volcano, hypocenters of B-type earthquakes are usually located in a cylindrical zone with a radius of about 200 m at depth of less than 3 km (e.g., 2 to 3.5 km for BH-type and less than 3 km for BL-type earthquakes) beneath the floor of the active Minamidake crater (e.g., Ishihara and Iguchi, 1989; Iguchi, 1989, 1994). Meanwhile, volcanic tremor episodes mostly take place near the active crater (e.g., Minakami et al., 1957; Kamo et al., 1977). Although our three-station observation cannot determine hypocenters precisely, we can roughly assume from these studies that both B-type earthquakes and volcanic tremor episodes are located in a narrow cylindrical zone beneath the floor of the active crater.

The spectra of two earthquakes (superscript of 'ref' as a reference event and 'k' as the kth event) recorded at a same station 'A' (given as subscript) are expressed by:

$$\begin{cases} O_{\mathrm{A}}^{\mathrm{ref}}(\omega) = S_{\mathrm{A}}^{\mathrm{ref}}(\omega) \cdot P_{\mathrm{A}}^{\mathrm{ref}}(\omega) \cdot R_{\mathrm{A}}^{\mathrm{ref}}(\omega) \\ O_{\mathrm{A}}^{k}(\omega) = S_{\mathrm{A}}^{k}(\omega) \cdot P_{\mathrm{A}}^{k}(\omega) \cdot R_{\mathrm{A}}^{k}(\omega) \end{cases} \quad (1)$$

where $O(\omega)$, $S(\omega)$, $P(\omega)$ and $R(\omega)$ are the spectra of the observed seismogram, of source characteristics, of wave-propagation effect along the path connecting the source and the receiver, and of recording-site effect, respectively. Assuming that the kth earthquake shares a common hypocenter with the reference event of a different magnitude, the spectral characteristics of the ray path $P(\omega)$ and the recording site $R(\omega)$ should be the same for both events.

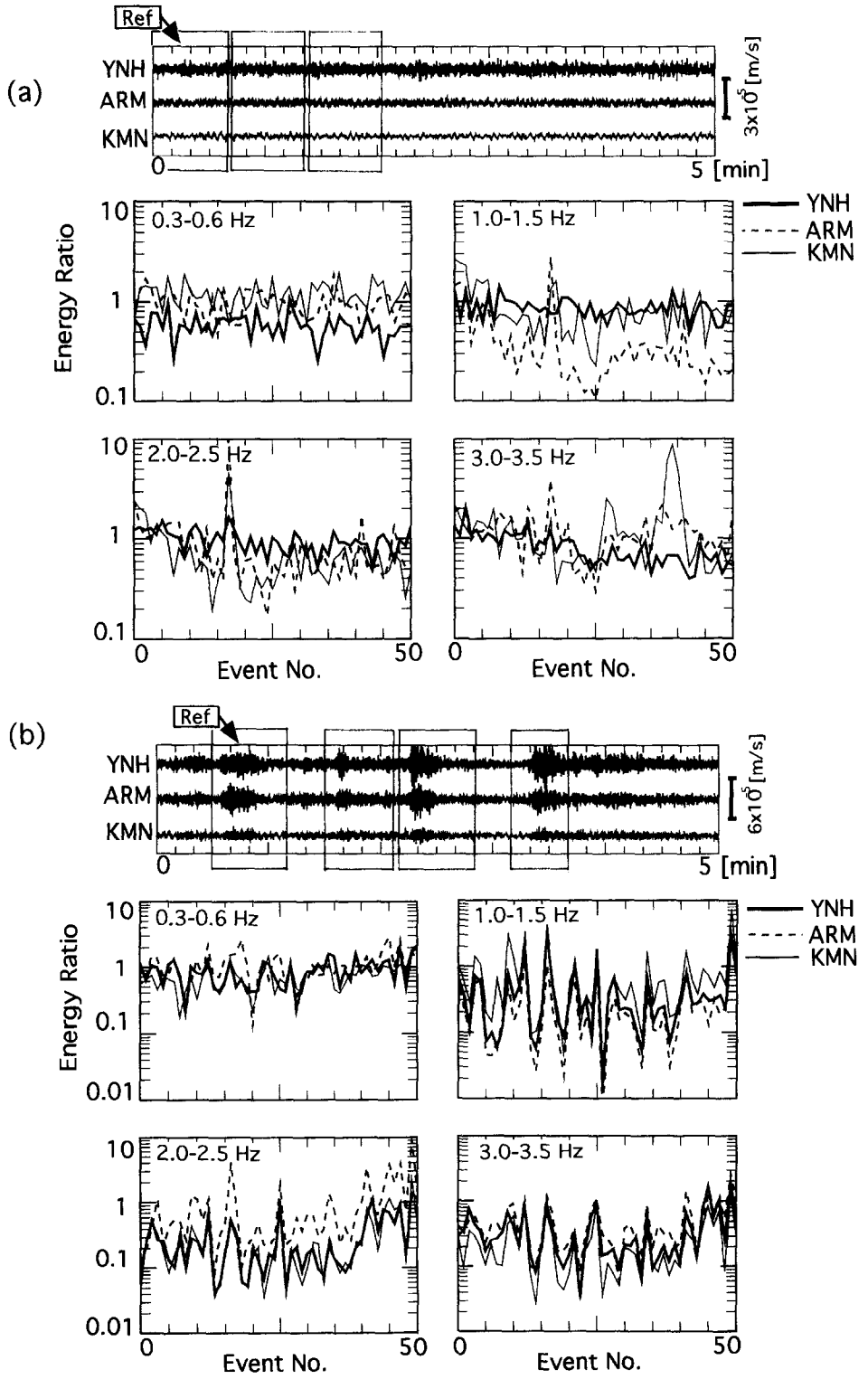
(a)
Ref
YNH
ARM
KMN
3x10⁵ [m/s]
0
5 [min]
Energy Ratio
10
1
0.1
0.3-0.6 Hz
1.0-1.5 Hz
2.0-2.5 Hz
3.0-3.5 Hz
YNH
ARM
KMN
0
Event No.
50
(b)
Ref
YNH
ARM
KMN
6x10⁵ [m/s]
0
5 [min]
Energy Ratio
10
1
0.1
0.01
0.3-0.6 Hz
1.0-1.5 Hz
2.0-2.5 Hz
3.0-3.5 Hz
YNH
ARM
KMN
0
Event No.
50

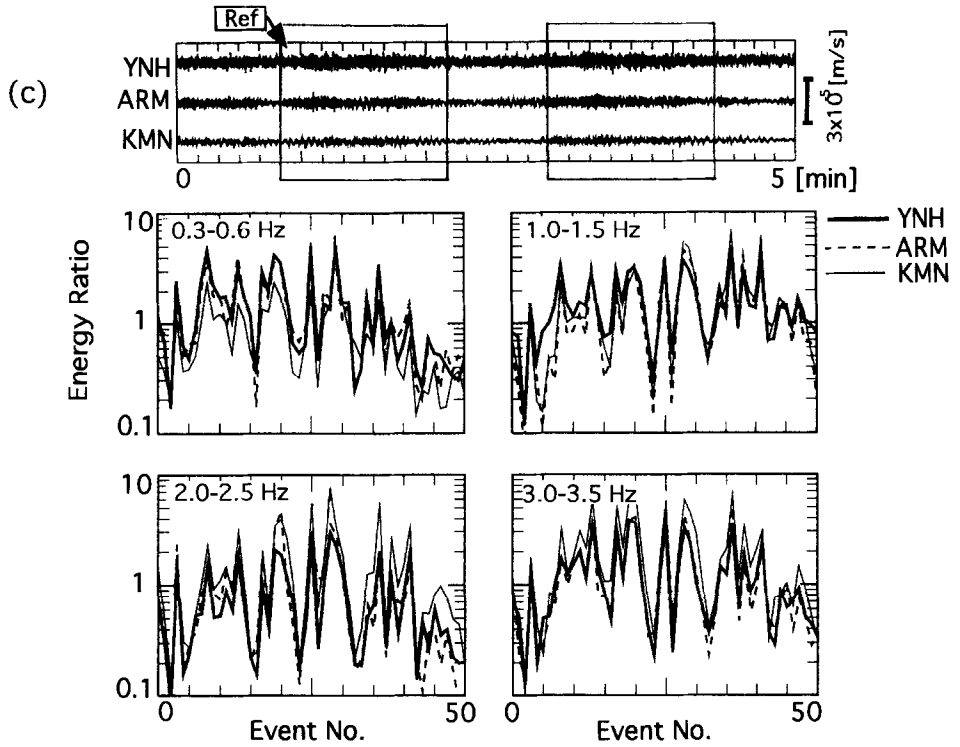

Fig. 4. Energy ratios of (a) background noise from 14:45 to 17:45 on February 25, (b) B-type earthquakes on January 25, and (c) volcanic tremor episodes on February 5–6. Preference data 'Ref' are indicated by an arrow. The data-window is selected to represent the recorded time length for each event. Spectral energy or power is integrated over four frequency ranges: 0.3–0.6 Hz, 1.0–1.5 Hz, 2.0–2.5 Hz, and 3.0–3.5 Hz.

Taking the spectral ratio f_{A_k} of the reference event and the kth event, we obtain:

$$f_{A_k} \equiv \frac{O_A^k(\omega)}{O_A^{ref}(\omega)} = \frac{S_A^k(\omega)}{S_A^{ref}(\omega)} \tag{2}$$

The similar observation at a different station B yields:

$$f_{B_k} \equiv \frac{O_B^k(\omega)}{O_B^{ref}(\omega)} = \frac{S_B^k(\omega)}{S_B^{ref}(\omega)} \tag{3}$$

If the above spectral ratio at the site B is same as that at the site A (i.e., $f_{A_k} = f_{B_k}$), we get:

$$\frac{S_A^k(\omega)}{S_A^{ref}(\omega)} = \frac{S_B^k(\omega)}{S_B^{ref}(\omega)} \tag{4}$$

implying the common spectral ratios of the source characteristics. If the relation Eq. (4) holds at any time-window during a sequence of B-type earthquakes or volcanic tremor episodes, the temporal variations of observed spectral properties can be attributed to source effect rather than to either path or site effect.

Instead of taking a spectral ratio at a single frequency, as shown in Eq. (4), we adopt the ratio of the energy (i.e., power spectrum) integrated over a finite frequency band including a spectral peak of B-type earthquakes or volcanic tremor episodes because actual spectral peaks cannot be defined by very narrow frequency bandwidths.

We first take energy ratio for background noise or a part of records without any events in the same frequency range as the one with spectral peaks of B-type earthquakes or volcanic tremor episodes. Four frequency ranges are selected: 0.3–0.6, 1.0–1.5, 2.0–2.5 and 3.0–3.5 Hz for 236 records with 41 s time-window from 14:45 to 17:45 on February 25. Fig. 4a shows the spectral ratios to f_0 as reference events at each site. The reference seismograms,

shown by the arrowed data-window in Fig. 4, are taken from 14:45:00 to 14:45:41.

We calculated correlation coefficients, r, for each pair of the spectral ratios Eq. (4) for the independence test among three sites. Correlation coefficient, r_{AB}, for n-pair of data $\{(f_{A_k}, f_{B_k})\}$ $(k = 1, 2, \ldots, n)$ is defined by:

$$r_{AB} \equiv \frac{S_{AB}}{\sqrt{S_A \cdot S_B}} \tag{5}$$

where

$$S_{AB} = n \sum_{k=1}^{n} f_{A_k} f_{B_k} - \sum_{k=1}^{n} f_{A_k} \sum_{k=1}^{n} f_{B_k} \tag{6}$$

and

$$S_B = n \sum_{k=1}^{n} f_{B_k}^2 - \left(\sum_{k=1}^{n} f_{B_k} \right)^2 \tag{7}$$

in which S_{AB} is called the covariance of data $\{(f_{A_k}, f_{B_k})\}$, and S_A and S_B are variances for f_{A_k} and f_{B_k}, respectively. Table 3 shows the averages of correlation coefficients for each pair (i.e., for ARM versus YNH, ARM versus KMN and KMN versus YNH). The values in all the frequency ranges, especially for 0.3–0.6 Hz, are small (e.g., $r = 0.051$–0.469), showing no correlation to each other. We confirm 'no correlation' by the χ^2-test that the ratio of three sites behave randomly with a level of significance $\alpha = 0.05$, and conclude that background noise do not share a common source. The recorded background noise has no characteristic spectral peaks in the frequency range from 1.0 to 3.5 Hz likely caused by any cultural activities. On the other hand, although some spectral peaks are noticed in the frequency range of 0.3–0.6 Hz, they were mainly caused by sea waves and wind (e.g., Tsuruga et al., 1994) and behave randomly at each site.

Table 3
Average of correlation coefficient

Frequency range	Background noise	B-type earthquakes	Volcanic tremor episodes
0.3–0.6 Hz	0.051	0.453	0.892
1.0–1.5 Hz	0.314	0.895	0.908
2.0–2.5 Hz	0.469	0.823	0.910
3.0–3.5 Hz	0.316	0.870	0.941

Next, we used an event at 20:05:30 on January 25 as a reference seismogram to study other B-type earthquakes on the same day with arbitrary time-length. Since the main spectral peaks of B-type earthquakes are in three frequency ranges (i.e., 1.0–1.5, 2.0–2.5 and 3.0–3.5 Hz), for which we calculated the energy ratios. To compare these signals with the background noise discussed above, another frequency range (0.3–0.6 Hz) is added where the dominant peaks of microseisms exist. The results for arbitrary 50 events are shown in Fig. 4b and correlation coefficients calculated for 127 events are given in Table 3. The coefficients in three frequency ranges from 1.0–1.5 Hz, 2.0–2.5 Hz and 3.0–3.5 Hz are significantly higher ($r > 0.84$) than for the lowest one, 0.3–0.6 Hz ($r < 0.50$). That is, spectral ratios in three frequency ranges including spectral peaks of B-type events behave coherently among three sites, ARM, YNH and KMN, while no clear correlations are found in the lowest frequency range with background noise. This suggests similar source locations and source mechanisms of B-type earthquakes during this period, and the observed spectral characteristics at each site mainly represent the source process.

Finally, we took an event at 22:04:50 of 40 s time-window as a reference seismogram to compare other volcanic tremor episodes on February 4 and 5, as shown in Fig. 4c. Correlation coefficients for 61 events are higher ($r > 0.89$) than those for B-type earthquakes in all the frequency ranges (Table 3). A χ^2-test indicated that the ratios in the higher three frequency ranges do not behave at random among three sites as for B-type earthquakes. We can conclude that the source location and the source mechanisms of volcanic tremor episodes are also common in our data set. The ratios in the lowest frequency range (0.3–0.6 Hz) also behave similarly to the other three ranges but at slightly random. Though it might be caused by some volcanic signals buried in the background noise, we cannot distinguish their signals visually because those amplitudes were as small as those of background noise.

In summary, the temporal variations of spectrals for both B-type earthquakes and volcanic tremor episodes in this study mainly reflect source mecha-

nisms, and the characteristics of site or path effects are minimal.

4. Temporal variations

During our observation, volcanic tremor episodes and a swarm of B-type earthquakes occurred from February 1 to 7, and on February 9 and 10 before several explosion earthquakes from February 8 to 11 (Fig. 3). Assuming that temporal and spatial variations are due to source effects, as discussed in the previous section, we analyzed the data of 352 B-type earthquakes on January 25 and 451 events on February 9, and volcanic tremor episodes on February 3 to 7 whose total duration time was about 1860 min. We discuss temporal variations of B-type earthquakes and volcanic tremor episodes in this section and spatial variations in the next section.

4.1. B-type earthquakes

A swarm of B-type earthquakes started at 18:42 on January 25 and culminated with an event at 21:26 with the maximum amplitude at ARM. Fig. 5 shows three-component seismograms and spectra of the largest B-type event. The maximum peak-to-peak amplitudes are about 1.0×10^{-4}, 3.0×10^{-4} and 2.7×10^{-4} m/s in up–down, north–south and east–west components, respectively. Three or four major spectral peaks exist in the frequency ranges of 1.1–1.3, 2.3–2.5, 2.5–2.8 and 3.4–3.6 Hz. The second major peak at 2.3–2.5 Hz has the largest total energy in all the components. For 352 B-type earthquakes, we calculate the running spectra with time-length of 5 s and time-shift of 1 s. To visualize temporal variations of the spectra, we contour the spectra in a time-frequency space, as shown in Fig. 6. The spectral amplitude of a given time-window in

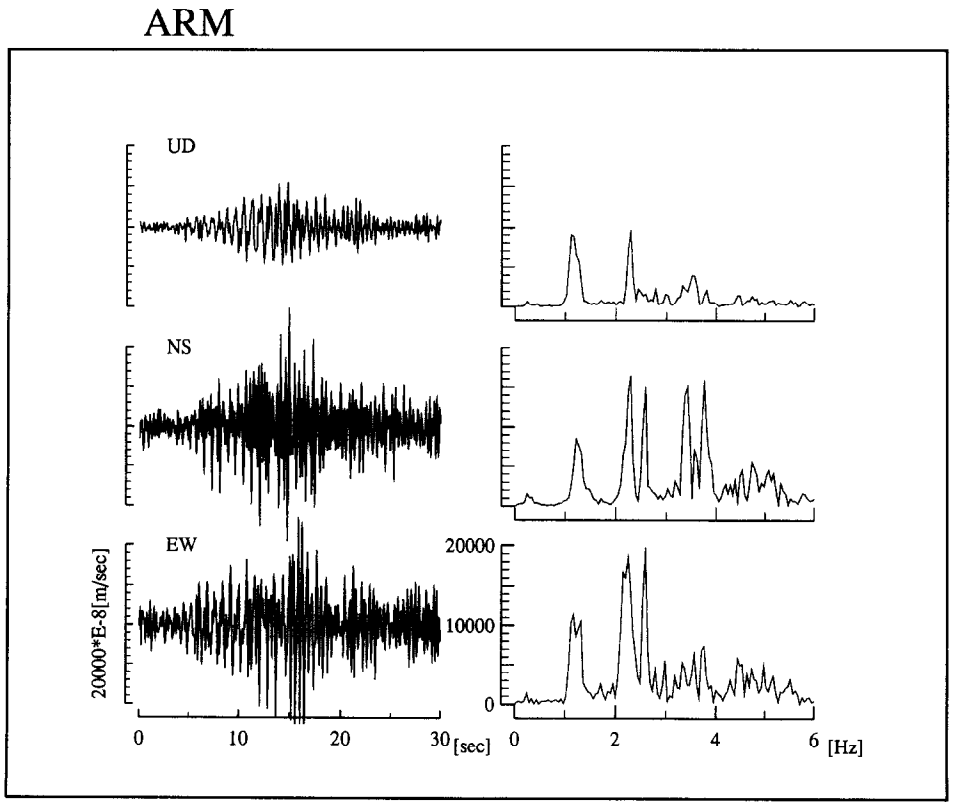

Fig. 5. Three-component seismograms and spectra of B-type earthquakes at 21:26 on January, 25. UD, NS and EW correspond to up–down, north–south and east–west components. Maximum peak-to-peak amplitudes are 1×10^{-4}, 3×10^{-4} and 3×10^{-4} m/s in the vertical, radial and horizontal component, respectively. Major spectral peaks are in the frequency ranges of 1.1–1.3, 2.3–2.5 and 3.4–3.6 Hz.

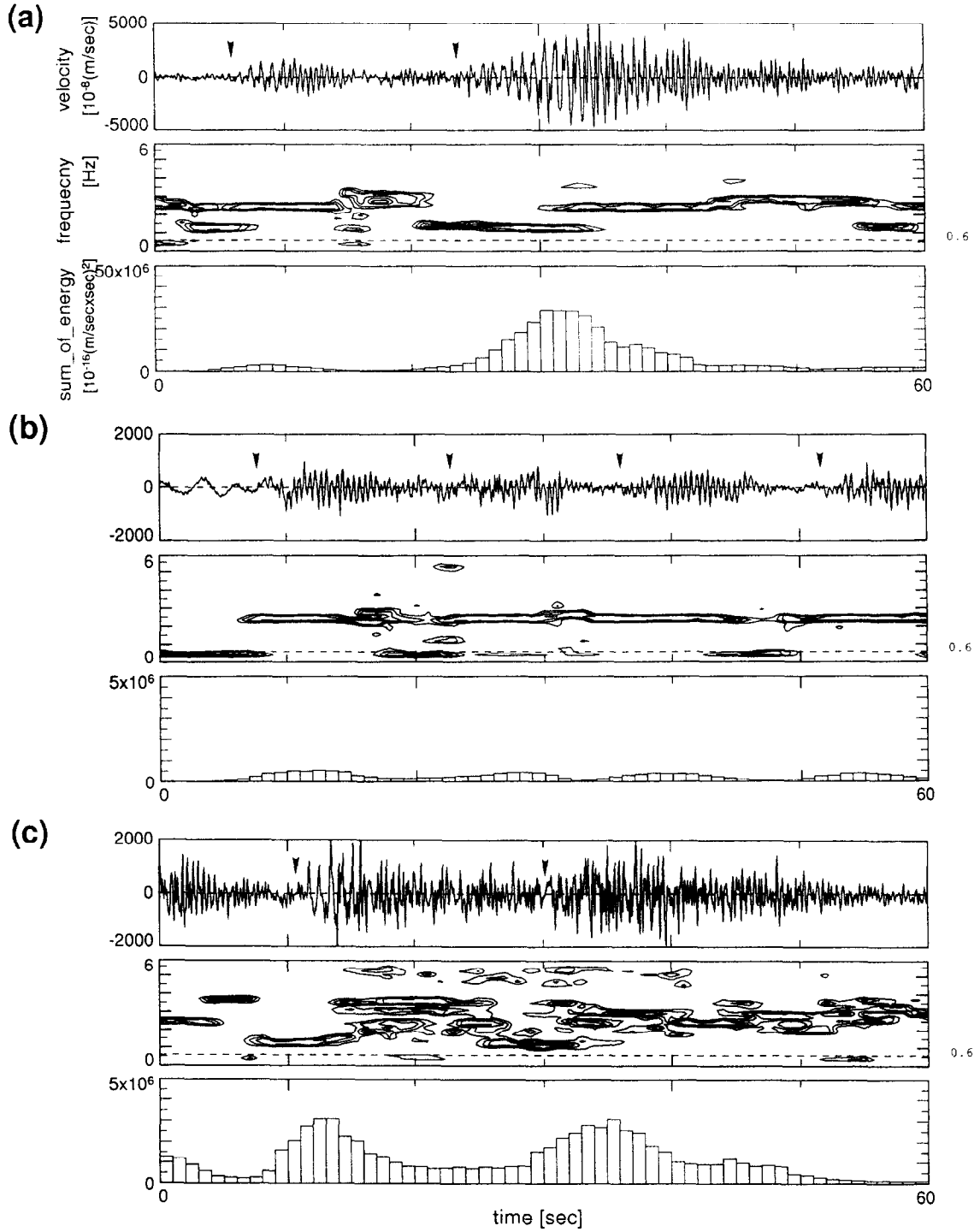

Fig. 6. Examples of three types of B-type earthquakes, B1, B2 and B3, in terms of temporal variation of major spectral peaks. An arrow denotes an onset of event.

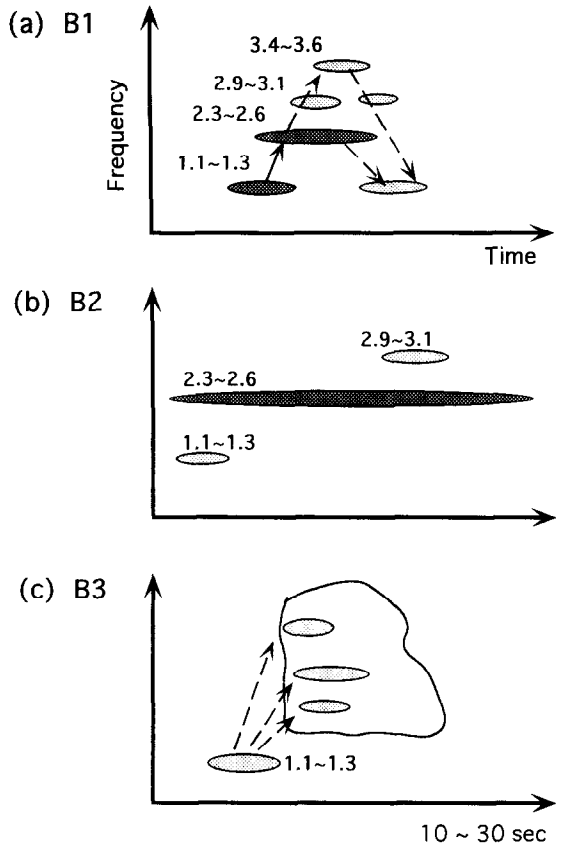

Fig. 7. Schematic views of the three types, B1, B2 and B3 events of Fig. 6.

this figure is normalized by the maximum value, in order to clearly observe the behavior of maximum peak frequencies. The energy integrated over the frequency range from 1 to 6 Hz is also obtained for each time-window. We can classify the analyzed 352 events into three types, called B1, B2 and B3 events, from the pattern of temporal variations. Fig. 6 gives a typical example of each type, schematically summarized in Fig. 7. The maximum spectral peak of B1 events is shifted from the lower frequency peak (1.1–1.3 Hz) to higher ones (2.3–2.5 and 3.4–3.6 Hz) with the interval of about 10 s. The maximum peak frequency varies in each time-window, but the

Table 4
Classification of B-type earthquakes

Event type	Frequency (event number)	Maximum energy for 5 s ($\times 10^{-16}$ (m/s·s)^2)
B1	73% (230)	$1-30\times10^6$
B2	20% (65)	$<5\times10^6$
B3	8% (26)	$1-5\times10^6$

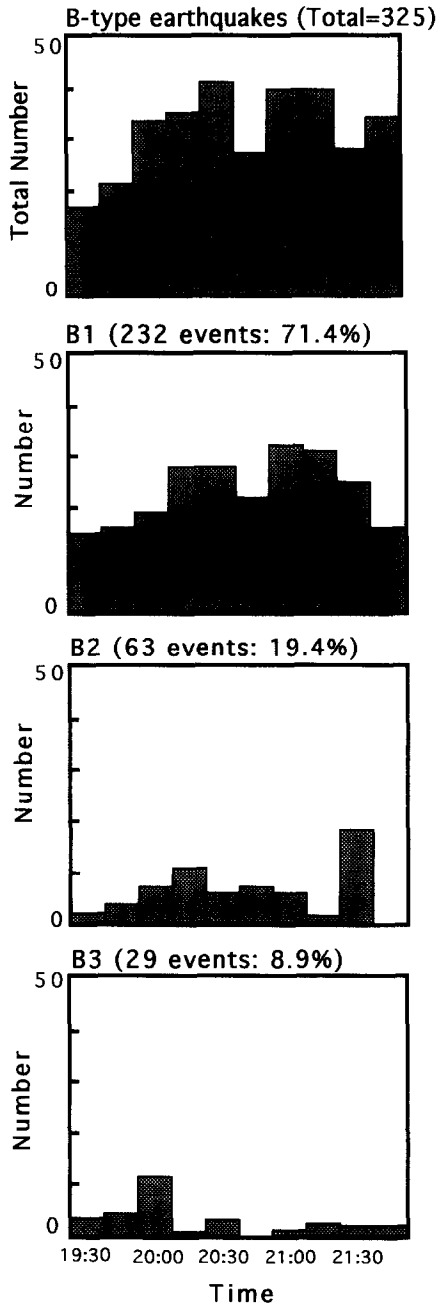

Fig. 8. Total numbers of B-type earthquakes and frequency of each type (B1, B2 and B3) for the period from 19:30 to 22:00 on January 25.

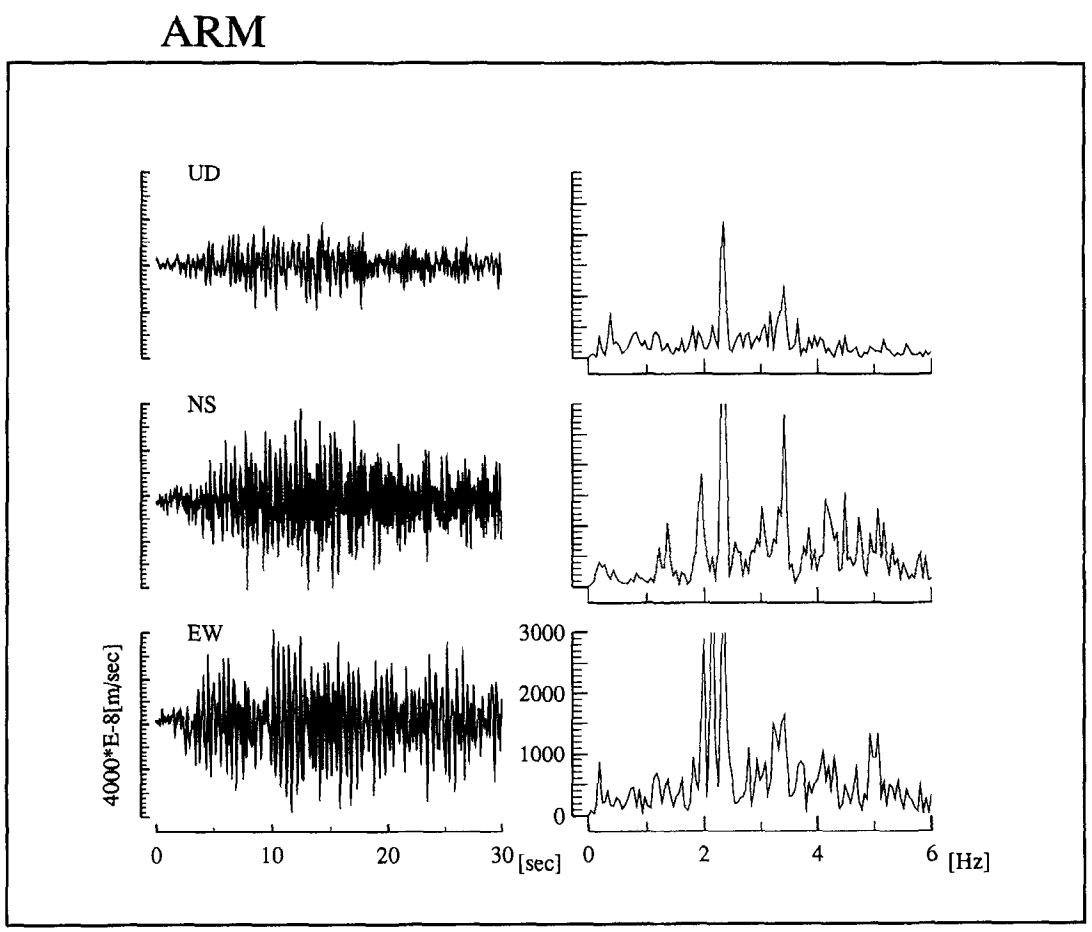

Fig. 9. Three-component seismograms and spectra of volcanic tremor episode at ARM at 5:31 on February 6. The maximum peak-to-peak amplitudes are about 2×10^{-5}, 6×10^{-5} and 5×10^{-5} m/s in vertical (UD), north–south (NS) and east–west (EW) components, respectively. Spectral peaks are in the frequency ranges of 1.1–1.3, 2.3–2.5 and 3.4–3.6 Hz.

main peak frequencies are nearly invariant even with significant variations of energy level. B2 events are characterized by one dominant spectral peak around 2.4 Hz and nearly monochromatic for 10–30 s. B3 events tend to start with one low-frequency peak (1.1–1.3 Hz) followed by the splitting into several peaks simultaneously. The frequency of their occurrences and the average of the maximum energy for each event are summarized in Table 4. Fig. 8 shows the numbers of B-type earthquakes from 19:30 to 22:00 on January 25. B1 events occurred most frequently when their amplitude is the largest, and B2 events appear to occur before and after B1 events. There are much fewer B3 events without any characteristic tendencies for their occurrence. Kakuta and Nonaka (1979) analyzed temporal variations of spectral peaks of volcanic earthquakes observed in the higher frequency range (> 2 Hz) at ARM and reported four types some of which can correspond to our three event types.

4.2. Volcanic tremor episodes

Many sequences of volcanic tremor episodes were recorded from February 1 to 7 before the swarms of B-type earthquakes on February 9. The maximum peak-to-peak amplitude of volcanic tremor episodes recorded at ARM on February 5–6 are about 2×10^{-5}, 4×10^{-5} and 4×10^{-5} m/s in the up–down, north–south and east–west components, respec-

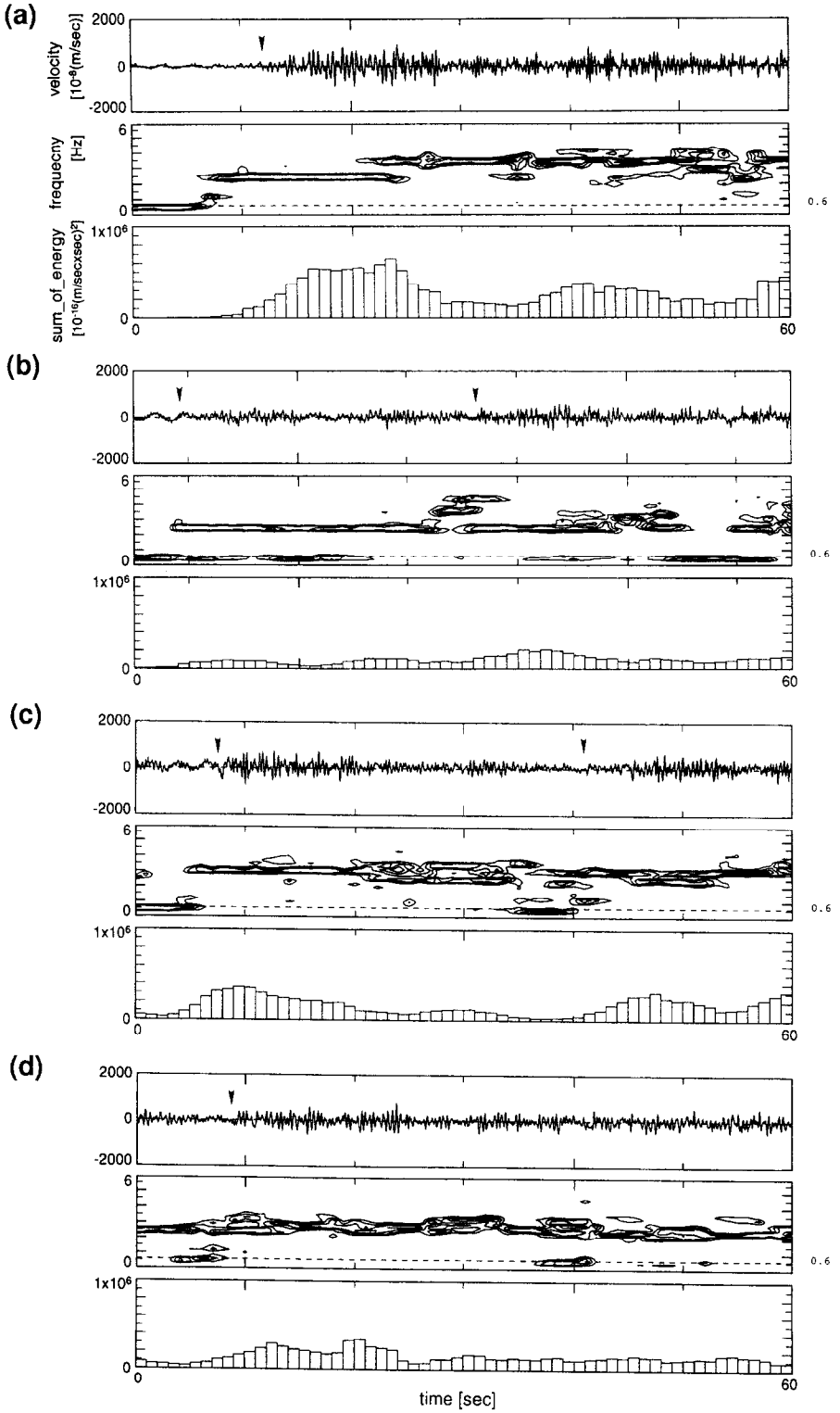

Fig. 10. Examples of four types of volcanic tremor episode, showing the temporal variations of maximum spectral peaks with their onsets denoted by arrows.

tively. Fig. 9 shows the three-component seismograms and the power spectra for a volcanic tremor episode recorded at ARM, starting at 5:31 on February 6. The main spectral peaks are located in the frequency ranges of 1.1–1.3, 2.3–2.5 and 3.4–3.6 Hz, similar to those of B-type earthquakes. The main peak frequencies are invariant but not for their intensities. Onsets of volcanic tremor episodes are not as clear as those of B-type earthquakes, comparable to background noise in some cases. We analyzed 99 events with clear spectral peaks on February 3–7. We can identify four types in terms of temporal variations of the maximum spectral peak, called T1, T2, T3 and T4 as for B-type earthquakes, as shown in Figs. 10 and 11. The maximum spectral peak of T1 events is shifted from a lowest main frequency (1.1–1.3 Hz or around 1 Hz) to higher ones (2.3–2.5 or 2.8–3.0 Hz and 3.4–3.6 Hz) with the interval of 10–30 s or more. Instead of gradual frequency shift, several spectral peaks seem to compete each other, resulting in temporal variation of spectral peaks. T2 events have one dominant peak around 2.4 or 3.0 Hz with minor lower and/or higher frequency peaks, or they are nearly monochromatic in some cases. The peak of T3 events starts at a relatively high frequency (2.9–3.1 Hz), then splits to both higher (3.4–3.6 Hz) and lower (2.3–2.6 Hz) frequencies. T4 events have several dominant spectral peaks around 2.4 or 3.0 Hz without one dominant peak. Table 5 lists the frequencies of occurrence and the maximum energy in the frequency range of 1–6 Hz for each type. T2 events take place most frequently with the largest energy.

Table 5
Classification of volcanic tremor episodes

Event type	Frequency (event number)	Maximum energy for 5 s ($\times 10^{-16}$ (m/s·s)^2)
T1	6% (6)	$0.4–2\times10^6$
T2	49% (48)	$0.1–1\times10^6$
T3	24% (24)	$<0.5\times10^6$
T4	21% (21)	$\approx0.4\times10^6$

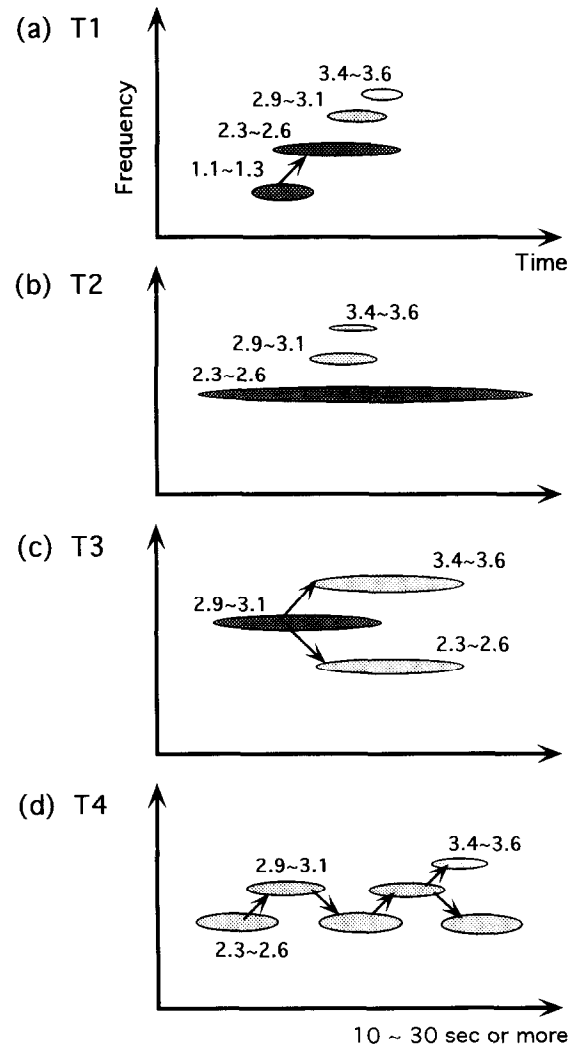

Fig. 11. Schematic views for T1, T2, T3 and T4 volcanic tremor episode of Fig. 10 on February 5 and 6.

Kamo et al. (1977) reported that major peak frequencies of volcanic tremor episodes at Sakurajima Volcano were 1.3 and 1.9 Hz, that are integer-multiples of the lowest peak frequency (0.65 Hz). In other words, each interval of three spectral peaks is same. The spectral peak became sharp as the dominant peak frequency decreased while the lowest peak frequency fluctuated in time between 0.9 and 1.8 Hz as well as the higher frequency peaks with maintaining the same interval in frequency. In our data set, the lowest peak (0.65 Hz) cannot be observed clearly. Higher spectral peak frequencies are nearly integer-multiples of the lowest frequency (about 1.2 Hz) or nearly equal interval of peak frequencies, similar to the observation of Kamo et al. (1977). However, the dominant peak frequencies are nearly constant in time even with various amplitude.

5. Spatial variations

In this chapter, we shall compare properties of B-type earthquakes and volcanic tremor episodes observed at four or three different sites. We mainly analyzed semi-continuous data recorded at three sites, ARM, YNH and KMN, and occasionally used triggered event data at KKM.

5.1. B-type earthquakes

We shall compare in seismograms of B-type earthquakes recorded at different sites. We define radial and transverse directions in the horizontal plane by assuming their hypocentral locations at the currently active Minamidake crater, judging from other seismic studies at Sakurajima Volcano (e.g., Kamo et al., 1977; Iguchi, 1994). Fig. 12 shows three-component seismograms and spectral amplitudes of a B-type earthquake recorded at 21:26 on January 25, which corresponds to the event shown in Fig. 5. The maximum amplitudes in the vertical, radial and transverse components are about 1.0×10^{-4}, 2.5×10^{-4} and 3.0×10^{-4} m/s at ARM, about 1.0×10^{-4}, 2.5×10^{-4} and 2.5×10^{-4} m/s at YNH, about 3×10^{-5}, 5×10^{-5} and 7×10^{-5} m/s at KMN, and about 1.0×10^{-4}, 1.0×10^{-4} and 1.0×10^{-4} m/s at KKM, respectively. The major three spectral peaks are found in frequency ranges of 1.1–1.3, 2.3–2.5 and 3.4–3.6 Hz for all the components. The lowest frequency peak exists at all the four sites while the other two higher peaks cannot be observed well at YNH, KMN and KKM. Although these spectral peak frequencies are shown to be caused by source process as mentioned in Section 3, the two higher spectral peaks might be attenuated through the path of wave propagating. Although spectral amplitude is rather high in a higher frequency range of 4–6 Hz at KKM, it could be caused by some site conditions such as traffics and constructions. Among four sites, peak frequencies are slightly different: the highest at YNH and the lowest at KMN and KKM. It seems to result from site characteristics of each observation site. Fig. 13 shows polarizations of a B-type earthquake recorded at 21:23, on January 25, 1993, especially classified as B1 that occurred most frequently and had a clearer onset than other types in our observation period. Top figure (a) shows original three-component seismograms, and center and bottom figures are bandpassed seismograms in a frequency ranges of (b) 2.0–2.5 Hz with their particle motions in both horizontal and vertical cross sections. Azimuth from the Minamidake crater to each site is represented by an arrow. Although it is not easy to identify accurate onsets of waves from our surface-site observation because of relatively large background noise, we identify three dominant phases polarized: (1) only in a vertical–radial cross section; (2) in a vertical–radial one with larger amplitude; and (3) in both vertical and horizontal cross sections, in two frequency ranges of 1.0–1.5 Hz and 2.0–2.5 Hz. The first phase shown in the first time-window of Fig. 13 polarizes linearly in the direction towards the Minamidake crater at ARM and YNH in the frequency range of 1.0–1.5 Hz and at all the sites in range of 2.0–2.5 Hz, behaving like P-wave motion. We notice that larger amplitude of 'second phase' appears in 1–2 s later in vertical–radial cross section at all the sites, similar to SV-wave. The third phase is found in the third time-window, after 3–5 s from an onset time. It includes a large transverse component such as SH- or Love wave motions. The early phases of B-type earthquakes mainly reflect source processes while the last phase might be caused by site characteristics because a direct Love wave should arrive earlier than this phase.

Other polarization studies (e.g., Kamo et al., 1977; Iguchi, 1985; Iguchi, 1994) also identified P, SV and SH waves in seismograms recorded at Sakurajima Volcano by borehole and array observations, roughly consistent with our results. Moreover, Iguchi (1989) reported that initial motions of BL-type earthquake in a swarm were compressional and dilatational arrivals with the ratio of 61% and 35%, respectively.

In summary, body waves with several spectral peaks (for 3–5 s after an onset) and results of other studies imply that spectral peak frequencies of B-type earthquake mainly reflect source process presented by a model such as cracks, explosion source and magma pocket oscillations over a conduit rather than a simple double-couple focal mechanism.

5.2. Volcanic tremor episodes

Fig. 14 shows three-component seismograms and spectral amplitudes of volcanic tremor episodes

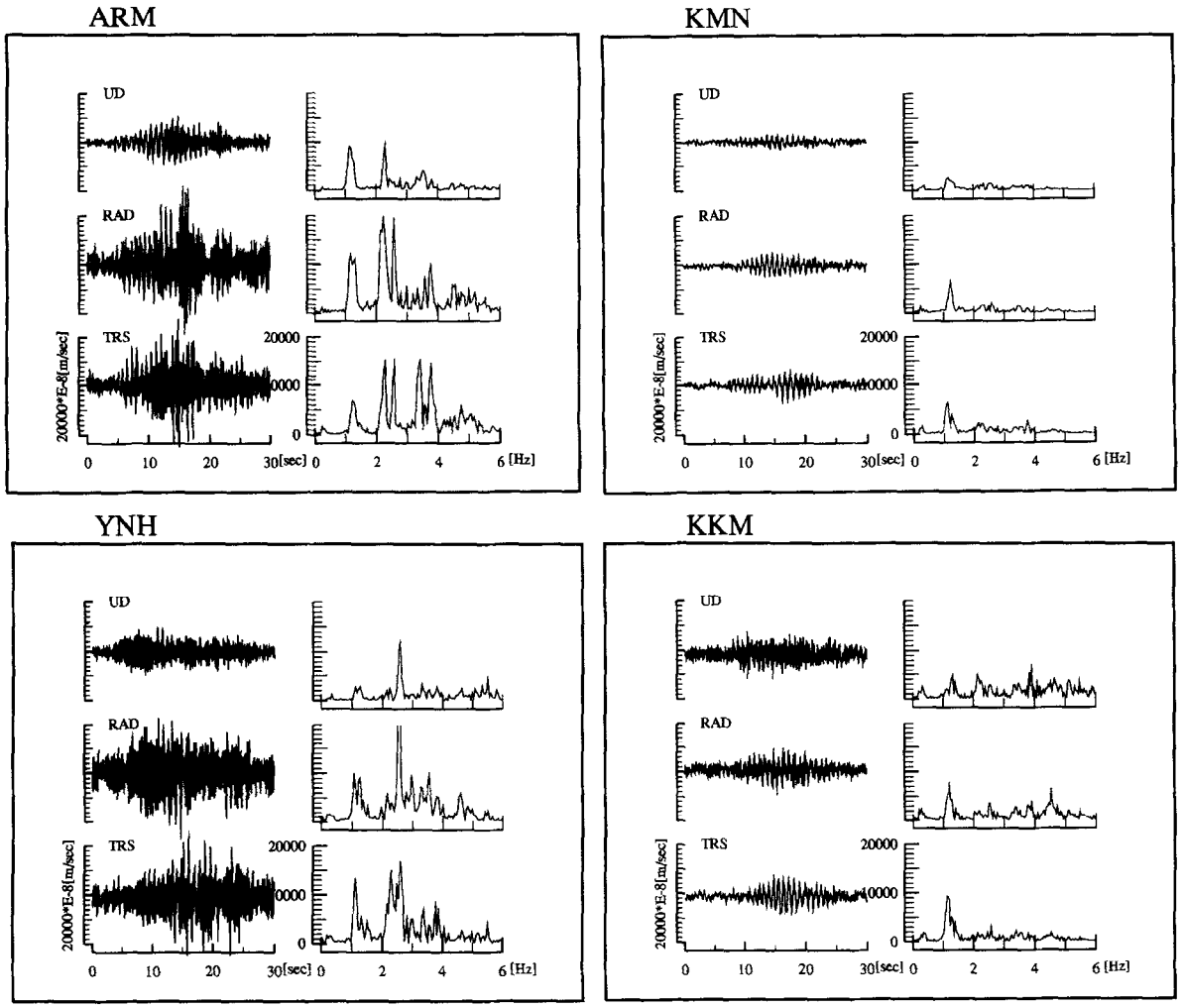

Fig. 12. Three-component seismograms and spectra of the B-type earthquake recorded at YNH, KMN and KKM at 21:26 on January 25, corresponding to the event in Fig. 5. UD, RAD and TRS correspond to the up-down, radial and transverse component, defined by assuming the location of the currently active Minamidake crater to be the hypocenter.

recorded at YNH and KMN starting at 5;31 on February 6, for the same tremor episodes shown in Fig. 9 at ARM. The maximum amplitudes in the vertical, radial, transverse components are about 3×10^{-5}, 5×10^{-5} and 5×10^{-5} m/s at YNH, about 2×10^{-5}, 6×10^{-5} and 5×10^{-5} m/s at ARM and about 5×10^{-4}, 1×10^{-5} and 1×10^{-5} m/s at KMN, respectively. The major spectral peaks exist in the frequency ranges of 1.1–1.3, 2.3–2.5 and 3.4–3.6 Hz. Fig. 15 shows polarizations of a volcanic tremor episode classified as a T1 event with large energy release, recorded at 05;36, on February 6, 1993. Three diagrams of particle motions in Fig. 15 correspond to an onset phase, large horizontal motions in

Fig. 13. (a) Original three-component seismograms of B-type earthquake recorded at 21:23 on January 25, 1993, at four sites, ARM, YNH, KMN and KKM, and polarizations in a frequency range of (b) 2.0–2.5 Hz. An arrow indicates an azimuthal direction from the Minamidake crater to each site. U, R and T correspond to the up, radial (+), and transverse (+) direction, respectively.

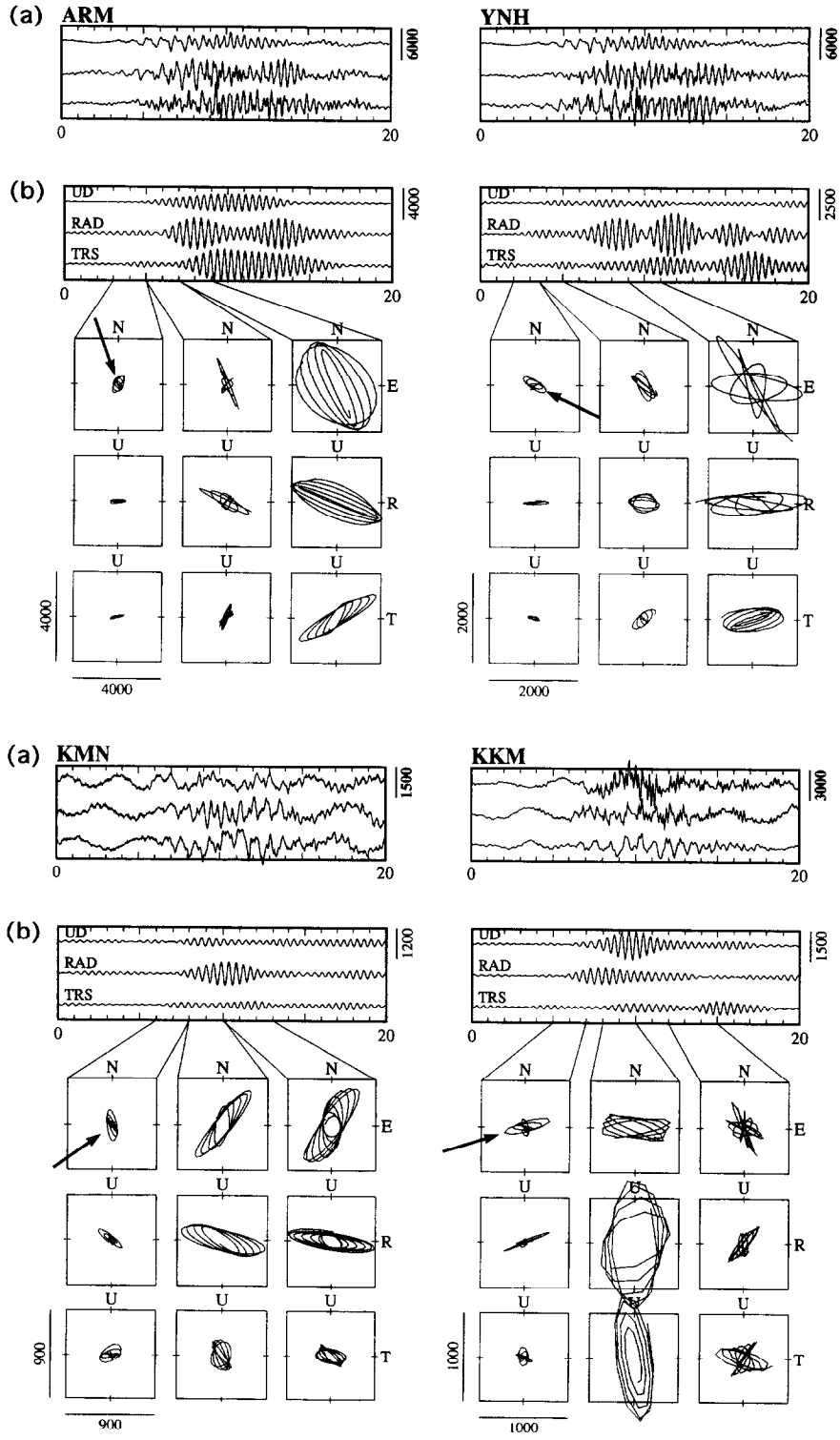
(a)
ARM
YNH
6000
0
20
(b)
UD
RAD
TRS
4000
2500
N
E
U
R
T
2000
4000
(a)
KMN
KKM
1500
3000
(b)
1200
1500
900
1000

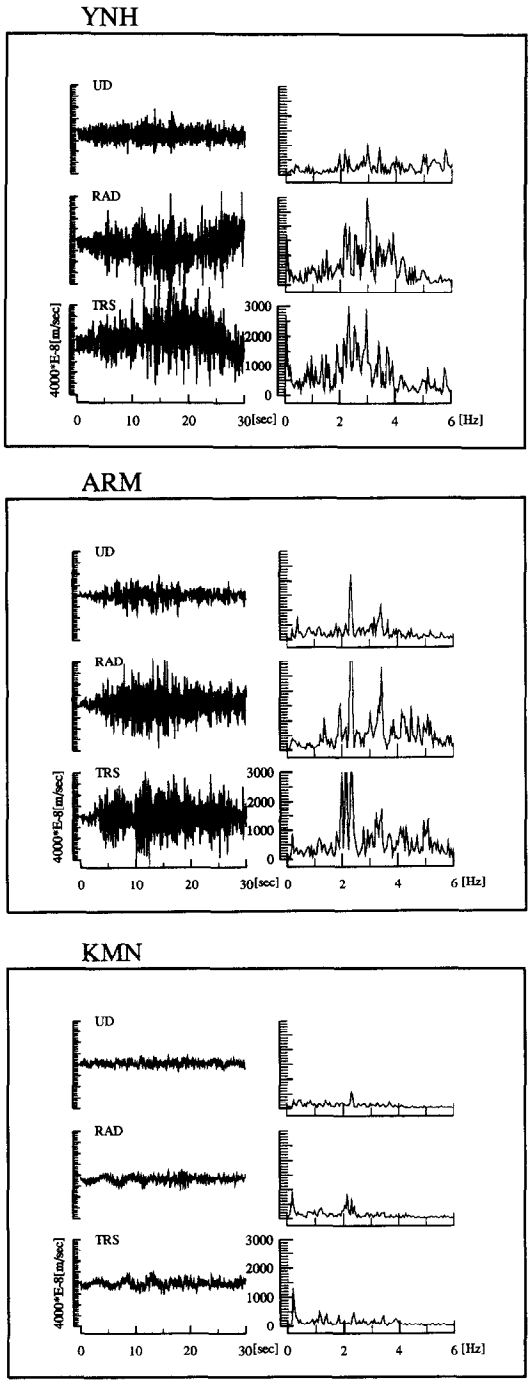

Fig. 14. Three-component seismograms and spectra of volcanic tremor episode recorded at YNH, ARM and KMN for the event shown in Fig. 9.

vertical–radial cross section and late large horizontal motions in the horizontal plane, called 'first', 'second' and 'third' phase, respectively. Dominant polarizations of the first and the second phases in the horizontal plane are roughly along the radial direction towards the crater or in vertical–radial plane, behaving like SV-waves. After 3–5 s (i.e., in the third time-window), early phases are superposed by dominant transverse motions, increasing as duration time of volcanic tremor episodes becomes larger.

Kamo et al. (1977) identified P- and SV-waves in seismograms of volcanic tremor episodes and concluded that dominant polarizations were different among oscillations of different spectral peaks. We could observe the same wave-type motions in our observation but, unlike the observation of Kamo et al. (1977), a clear tendency of polarizations in all the selected frequency ranges with spectral peaks.

These results are similar to those of B-type earthquakes, and early phases of volcanic tremor episodes mainly reflect source processes and the later one might be caused by site characteristics.

6. Relation between B-type earthquakes and volcanic tremor episodes

The temporal and spatial variations of spectral peaks for B-type earthquakes and volcanic tremor episodes exhibit many common features as shown in the previous two sections. This implies that both types of activity may share the common source location and source mechanism. Here we discuss the relationship between these two types of volcanic earthquakes.

We found three types of B-type earthquakes and four of volcanic tremor episodes in terms of temporal variations of spectral peaks (Figs. 6 and 10). Here, we neglect B3, T3 and T4 events because of their rare occurrences. The maximum spectral peaks of both B1 and T1 events are shifted from one frequency peak (1.1–1.3 Hz) to a higher one (2.3–2.5 Hz) in the time interval of about 10 s. On the other hand, both B2 and T2 events have a similar dominant peak around 2.4 Hz in the duration time of 10–30 s. Tables 4 and 5 imply that the difference between B-type earthquakes and volcanic tremor episodes is related only with output energy, other-

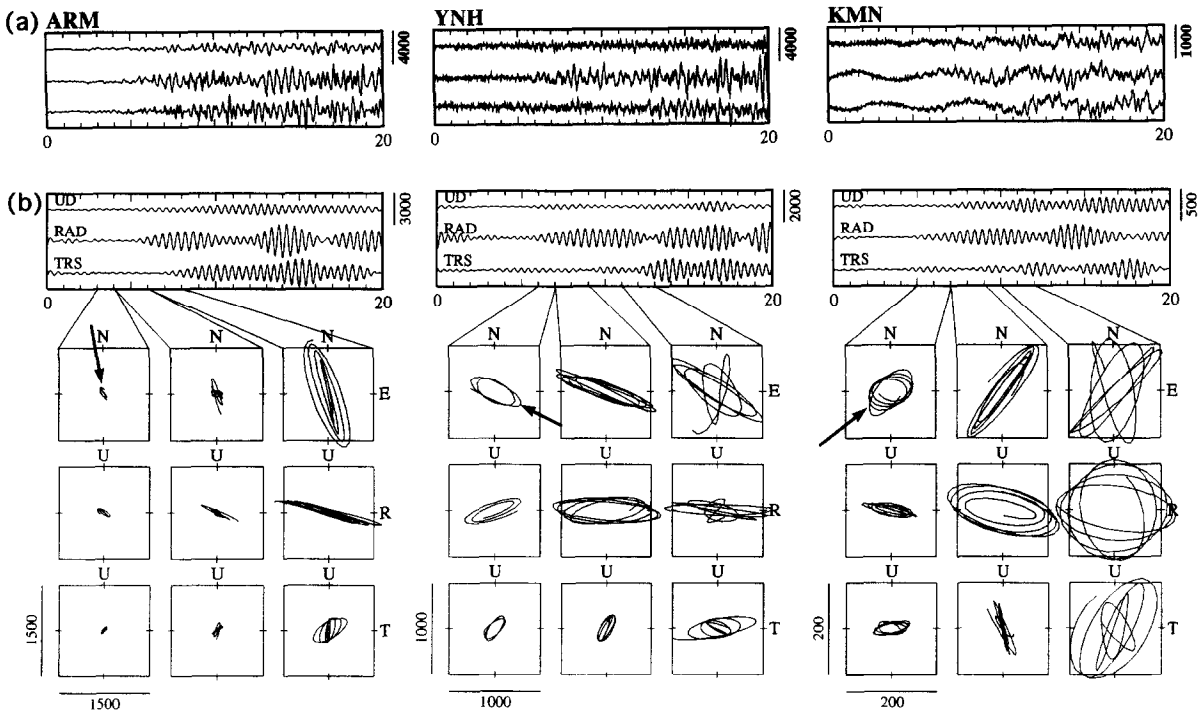

Fig. 15. Same as Fig. 13 except for the volcanic tremor episode recorded at 21:23 on January 25, 1993, at three sites, ARM, YNH and KMN.

wise they should share same characters. Fig. 16 shows relationship between maximum energy density and duration time of a single subevent for B-type earthquakes, volcanic tremor episodes and explosion earthquakes with a straight line fitted by the least-square method in the log–log scale. The maximum energy is defined by the peak rake of integrated energy, as described in Section 4, while the time interval to define a half the maximum energy represents the duration time here. If two or more energy peaks are overlapped, we simply define the duration time by the total duration time divided by the number of peaks, as shown in the bottom of Fig. 16. Although there are some scatters in data, particularly volcanic tremor episodes probably due to complex and continuous pattern of their occurrence (i.e., B2 or T2 events) rather than isolated individual events (i.e., B1 or T1 events), these three types of volcanic events have a nearly constant duration time around 10 s for each subevent despite their wide coverage of energy level. This strongly implies that all the above types of volcanic event has some common characters in their source processes with different energy levels of activity.

We summarize temporal variations of spectra for B-type earthquakes and volcanic tremor episodes in Fig. 17, as the total energy of a single subevent increases from the bottom to the top. The B1 events have the highest energy and the T2 have the lowest of these four types. When a seismic source radiates relatively large energy (about 10 times of volcanic tremor episodes), we generally observe a B-type earthquake characterized by a B1 event. In contrast, for the minimum energy radiation, we observe a volcanic tremor episode classified as a T2 event. Since spectral peaks of B-type earthquakes and volcanic tremor episodes are located in the same frequency range (1.1–3.6 Hz) and their temporal behaviors are similar in the time interval of 10–30 s, which corresponds to the total interval of one sequence, we can conclude that B-type earthquakes and volcanic tremor episodes share a common source mechanism, but their apparent difference is only due to the difference in total energy and total duration

time. If we assume that both B-type earthquakes and volcanic tremor episodes consists of a sequence of many sub-events, this study strongly support the idea that these subevents cover an extremely wide range of energy level but with nearly constant duration time ($\sim$ 10 s) and peak frequency range (1.1–3.6 Hz). Our study alone cannot pin-point the concrete source mechanism of these events, but the alone conclusion provides some important constraints on possible source processes. For example, the resonance inside a simple magma body such as one crack cannot explain the nearly constant duration time

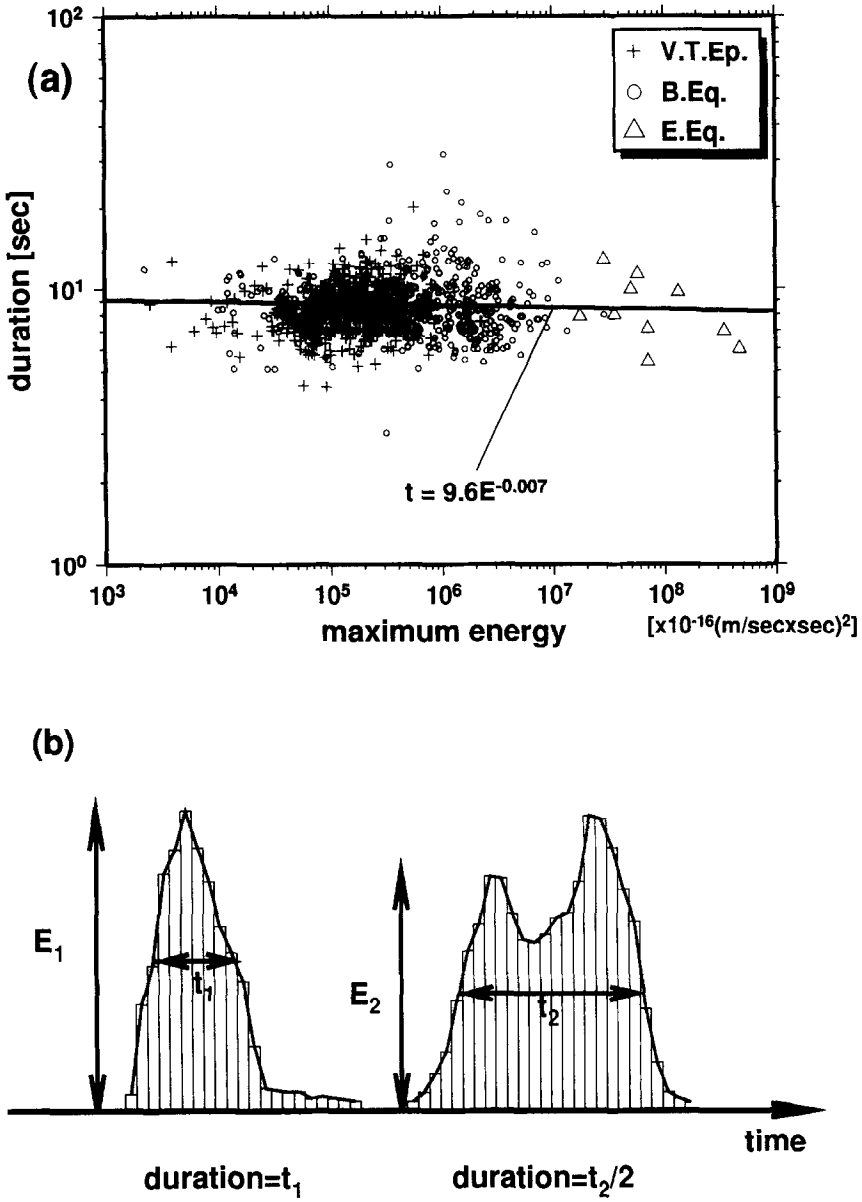

Fig. 16. (a) Plot of maximum energy versus duration time of a single subevent for B-type earthquakes, volcanic tremor episodes and explosion earthquakes with a least-square fitted straight line, and (b) definition of the maximum energy (E_1 or E_2), the total duration time (t_1 or t_2) and the number of subevents.

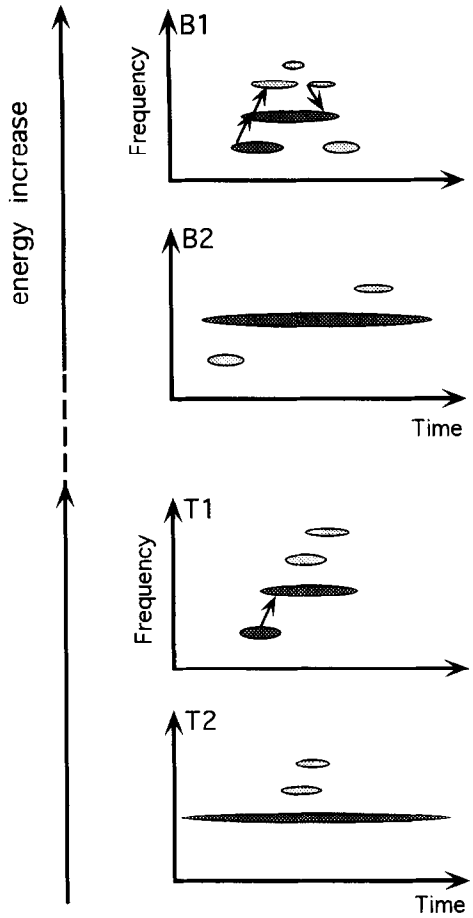

Fig. 17. Comparison of temporal variations of B-type earthquakes and volcanic tremor episode, as relative energy increases from the bottom to the top.

regardless of its energy level if decay is due to intrinsic attenuation of fluid inclusion in the body. Any complex interactions among plural bodies such as cracks connected each other are required, including the possibility non-linear effect (e.g., Ferrazzini et al., 1990; Honda and Yomogida, 1993).

7. Conclusions

We conducted broadband seismic observation at three sites around the Sakurajima Volcano from December 1992 to March, 1993. We used three STS-2 seismometers, recording in the frequency range from 0.03 to 6 Hz, in order to clarify spatial and temporal variations of spectral properties of volcanic earthquakes such as B-type earthquakes and volcanic tremor episodes. We carefully analyzed the data of B-type earthquakes on January 25 and volcanic tremor episodes from February 5 to 6, prior to three explosion earthquakes on February 9 and 10.

First, we conclude that spectral peaks of B-type earthquakes and volcanic tremor episodes mainly reflect source characteristics rather than path or site effect in the terms of the consistencies of spectral peak frequencies among all the sites and body-wave propagation in an early part of seismograms. Similarities in the temporal variation of spectral properties indicate that B-type earthquakes and volcanic tremor episodes share common source mechanism but not the same energy radiation.

Since volcanic tremor episodes tend to take place prior to swarms of B-type earthquakes and/or stronger explosion earthquakes, we can summarized one eruption sequence as follows: in the early stage energy radiation is weak, creating volcanic tremor episodes, as the radiated energy increase, seismic activity shifts from volcanic tremor episodes to B-type earthquakes but source location and source mechanism are nearly same. The occurrence of B-type earthquakes gradually increases, followed by the final explosion earthquakes with summit eruptions.

Next important step is to reveal the source mechanism of B-type earthquakes and volcanic tremor episodes. Broadband seismic observation with many stations are recommended, including array observation. Still, site and path effects must be clearly removed in these studies, and precise evaluation of these effects should be conducted by several borehole seismic observations in future.

Acknowledgements

We are grateful to Vaclav Vavrycuk of for careful reviews of the manuscript. We appreciate Yasuto Kuwahara, Hirotoshi Matsubayashi and Takashi Kato for their supports in the field experiments and many helpful technical advices. We also thank the cooperation of Kagoshima University, the Kagoshima meteorological observatory of the Japan Meteorological

Agency, the city of Kagoshima and the town of Sakurajima, for offering three temporary observation sites in this study. We also thank Yasuyuki Iwase, Takamoto Okudaira and Yoko Tono for their helpful comments. We sincerely thank Dr. Steve Malone and anonymous reviewer for constructive review of the manuscript. A part of this study was supported by a Grant-in-Aid for Scientific Research from the Ministry of Education, Science and Culture of Japan.

References

Aramaki, S. and Kobayashi, T., 1986. Chemical composition of the volcanic products from Aira caldera and Sakurajima volcano, with special reference to An-ei eruption. Rep. 5th Joint Obs. Sakurajima Volcano, pp. 115–129 (in Japanese).

Berckhemer, H., 1962. Die Ausdehnung der Bruchfläche im Erdbebenherd und ihr Einfluss auf das seismische Wellenspektrum, Gerlands. Beitr. Geophys., 71: 5–26.

Eto, T., 1988. Predictive phenomena of volcanic eruptions at Sakurajima volcano. Bull. Volcanol. Soc. Jpn., Ser. 2, 33: 104–106 (in Japanese).

Ferrazzini, V., Chouet, B., Fehler, M. and Aki, K., 1990. Quantitative analysis of long-period events recorded during hydrofracture experiments at Fenton Hill, New Mexico. J. Geophys. Res., 95: 21,871–21,884.

Fukuyama, H. and Ono, K., 1981. Geological map of Sakurajima volcano. Geol. Surv. Jpn. (in Japanese).

Goldstein, P. and Chouet, B., 1994. Array measurements and modeling of sources of shallow volcanic tremors at Kilauea volcano, Hawaii. J. Geophys. Res., 99: 2637–2652.

Honda, S. and Yomogida, K., 1993. Periodic magma movement in the conduit with a barrier: A model for the volcanic tremor. Geophys. Res. Lett., 20: 229–232.

Iguchi, M., 1985. Analysis of volcanic shallow earthquakes observed near the active crater. Bull. Volcanol. Soc. Jpn., Ser. 2, 30: 1–10 (in Japanese with English abstract).

Iguchi, M., 1989. Distribution of the initial motions of volcanic microearthquakes (B-type) at Sakurajima volcano. Ann. Disast. Prev. Res. Inst., Kyoto Univ, 32B-1: 13–22 (in Japanese with English abstract).

Iguchi, M., 1994. A vertical expansion source model or the mechanisms of earthquakes originated in the magma conduit of an andesitic volcano: Sakurajima, Japan. Bull. Volcanol. Soc. Jpn. Ser. 2, 39: 49–67.

Ishihara, K. and Iguchi, M., 1989. The relationship between micro-earthquake swarms and volcanic activity at Sakurajima volcano. Ann. Disast. Prev. Res. Inst., Kyoto Univ, 32B-1: 223–29 (in Japanese with English abstract).

Kakuta, T. and Idegami, Z., 1970. The volcanic tremors of C-type at the Sakurazima volcano. Bull. Volcanol. Soc. Jpn., Ser. 2, 15: 61–74 (in Japanese with English abstract).

Kakuta, T. and Yoshiyama, R., 1977. Seismological investigation of the events occurred in Sakurajima volcano, analysis of seismic data from stations at various elevations. Bull. Volcanol. Soc. Jpn, Ser. 2, 22: 1–12 (in Japanese with English abstract).

Kakuta, T. and Nonaka, Y., 1979. Spectra of volcanic earthquakes related to the eruptions of Sakura-jima volcano in February, 1975. Bull. Volcanol. Soc. Jpn., Ser. 2, 24: 213–222 (in Japanese with English abstract).

Kamo, K., 1978. Some phenomena before the summit eruptions at Sakura-zima volcano. Bull. Volcanol. Soc. Jpn., Ser. 2, 23: 53–64 (in Japanese with English abstract).

Kamo, K., Furusawa, T. and Akamatsu, J., 1977. Some natures of volcanic micro-tremors at the Sakura-jima volcano. Bull. Volcanol. Soc. Jpn., Ser. 2, 22: 41–58 (in Japanese).

Kawakatsu, H., Ohminato, T., Ito, H., Kuwahara, Kato, T., Tsuruga, K., Honda, S. and Yomogida, K., 1992. Broadband seismic observation at the Sakurajima volcano, Japan. Geophys. Res. Lett., 19: 1959–1962.

Minakami, T., 1960. Fundamental research for predicting volcanic eruption (Part 1). Bull. Earthq. Res. Inst., 38: 497–544.

Minakami, T., Mogi, K., Hiraga, S. and Miyazaki, T., 1957. On the investigation of explosive activities of Sakura-zima and various earthquakes originating from the volcano. Bull. Volcanol. Soc. Jpn. Ser. 2, 2: 77–90 (in Japanese with English abstr.).

Mori, J., Patia, H., McKee, C., Itikarai, I., Lowenstein, P., Desaintours, P. and Talai, B. 1989. Seismicity associated with eruptive activity at Langila volcano, Papua New Guinea. J. Volcanol. Geotherm. Res., 38: 243–255.

Nishi, K., 1966. High Sensitivity seismometric observation near the crater of volcano Sakurajima. (Part I) On the initial motion of B type volcanic micro-earthquake, Bull. Volcanol. Soc. Jpn., Ser. 2, 11: 84–92 (in Japanese with English abstract).

Nishi, K., 1978. On the focal mechanism of volcanic earthquakes in Sakurajima volcano. Ann. Disast. Prev. Res. Inst., Kyoto Univ., 21B-1: 145–152 (in Japanese with English abstract).

Ohminato, T., Ito, H., Kuwahara, Y., Kawakatsu, H., Kato, T. and Tsuruga, K., 1993. Observation at Sakurajima volcano, Japan. Abstr. Seismol. Soc. Jpn., 2: 205 (in Japanese).

Schick, R., Lambardo, G. and Patane, G., 1982. Volcanic tremors and shocks associated with eruptions at Etna (Sicily), September 1980. J. Volcanol. Geotherm. Res., 14: 261–279.

Tsuruga, K., Yomogida, K., Honda, S., Ito, H., Kawakatsu, H. and Ohminato, T., 1994. Observation of microtremors in the Tsukuba Area, Japan, using a portable broadband seismometer. J. Sci. Hiroshima Univ., Ser. C, 10: 1–9.

Tsuruga, K., Honda, S., Yomogida, K., Ito, H., Ohminato, T., Eguchi, T. and Fujita, E., 1995. 1994 multi-site broadband seismic observation at Sakurajima volcano, Japan. J. Sci. Hiroshima Univ., Ser. C, 10: 193–197.